

Chapter 8

Use of TTCF to calculate the viscosity in a weak field

8.1. Introduction

The study of the relationship between the pressure tensor and shear rate in a shear flow has both theoretical and practical significance, and is one of the most prominent topics in rheology. The response at a small field is especially important, because most experiments in the laboratory and most industrial processes occur in the small field region. Mode coupling theory [Kaw93] also predicts an asymptotic behaviour in zero field limit.

It is well known that direct nonequilibrium molecular dynamics (NEMD) is very effective for strong fields. However, in the small field limit, direct time-averaging NEMD suffers from poor signal-to-noise ratios. Alternatively, one can use the Green-Kubo relations [Kub57, Ald57] to calculate shear viscosity in the linear regime. This method calculates transport coefficients by observing the fluctuations of interesting quantities in an equilibrium state. Transport coefficients can be obtained by time integration of an autocorrelation function. But the main problem with the Green-Kubo method is that the correlation functions decay with time very slowly, and are believed to exhibit a $t^{-3/2}$ long time tail [Ald69, Ald70]. The other limitation on the Green-Kubo method is that it is restricted to the linear regime. For long chain molecules, for example, nonlinear effects may be important when in the weak field limit. In such a case, the Green-Kubo approach could not help.

In order to overcome these limitations, the transient time correlation function method (TTCF) was proposed by Evans and Morriss [Eva88, Mor87] in the 1980s. It is a nonlinear

response theory and plays a role as a bridge between nonequilibrium molecular dynamics and the Green-Kubo relations because it can be used in both the strong field and weak field limit, although it is not as efficient as NEMD at strong fields. Evans and Morris proved its correctness by comparing TTCF calculations with direct time-averaging. Todd [Tod97b] applied TTCF to simulate elongational flow and found it was efficient at low strain rates. Borzak, *et al*, [Bor02], used TTCF to study the shear viscosity of a simple fluid over a wide range of shear rates.

In this chapter we will apply TTCF to simulate planar Couette flow of the Weeks-Chandler-Andersen (WCA) [Wee71] fluid. Our objectives are to study the range of field strengths over which TTCF is more effective than direct NEMD, and to examine the decay of the stress autocorrelation function. Our intention had also been to examine the mode coupling theory predictions in the weak field limit but we were unable to obtain suitably good data.

8.2. Methodology

In TTCF, an arbitrary phase variable B can be calculated by a transient time correlation function [Eva90]:

$$\langle B(t) \rangle = \langle B(0) \rangle - \beta F_e \int_0^t ds \langle B(s) J(0) \rangle \quad (8.1)$$

where $\beta = 1/kT$, k is Boltzman's constant, T is temperature, F_e is external field and J is the dissipative flux. The angular bracket $\langle \rangle$ means a time average. We notice that the above correlation function connects a nonequilibrium phase variable B at some time t with the equilibrium dissipative flux at the start time.

In the case of planar Couette flow, J is the shear stress P_{xy} times the system volume V , and F_e is shear rate $\dot{\gamma}$. The above formula therefore becomes:

$$\langle B(t) \rangle = \langle B(0) \rangle - \beta \dot{\gamma} V \int_0^t ds \langle B(s) P_{xy}(0) \rangle \quad (8.2)$$

As Eqn. (8.2) contains the value of a nonequilibrium phase variable at time s , we still need to run nonequilibrium trajectories. To run these trajectories, we still use the standard thermostated SLLOD equations of motion and Lees-Edwards boundary conditions [Eva90]. In our work, we use the fourth-order Runge-Kutta method to solve the equations of motion stepwise. This method is used because it is entirely self-starting, ensuring that all correlations are accurate.

To apply TTCF to the studied system, we run a long equilibrium trajectory. At equal intervals along this equilibrium trajectory, we take the equilibrium phase point as a starting point and initiate a pair of nonequilibrium trajectories. We then average over these nonequilibrium trajectories to get the transient time correlation functions. Furthermore, using mapping techniques [Eva90] we can obtain two or more starting points from one phase point. The use of such mappings also improves the statistical accuracy of the data as discussed in Chapter 4 [Eva90]. In our work we use the y-reflection mapping [Eva90]:

$$(\mathbf{x}, \mathbf{y}, \mathbf{z}, \mathbf{p}_x, \mathbf{p}_y, \mathbf{p}_z) \rightarrow (\mathbf{x}, -\mathbf{y}, \mathbf{z}, \mathbf{p}_x, -\mathbf{p}_y, \mathbf{p}_z) \quad (8.3)$$

Our atoms interact via the WCA potential, which can be expressed by Eqn. (4.6).

We let the WCA potential constants σ , ϵ , the atomic mass and Boltzmann's constant to be unity. Thus all the quantities are expressed in reduced units and we omit the asterisk symbols for convenience.

Unless otherwise mentioned, all the simulations are performed close to the Lennard-Jones triple point, $(T, \rho) = (0.722, 0.8442)$. The potential cutoff distance is $2^{1/6}$. We use integration time steps of 0.001 or 0.002. Nonequilibrium trajectories are initiated at intervals of 2500 time steps along the equilibrium trajectory.

8.3. Comparison between direct NEMD and TTCF

In Figures 8.1 (a--g), we plot the simulation results of both direct NEMD and TTCF at a shear rate $\dot{\gamma} = 1$. They include elements of the pressure tensor, isotropic pressure, energy and viscosity respectively, and are computed for a 256 particle system. We run 10 equilibrium trajectories of 2500×10000 time steps length from different initial conditions. From every equilibrium trajectory we can initiate 20000 nonequilibrium trajectories. Each nonequilibrium trajectory is 2000 time steps long. Here the time step is 0.001. The final results are obtained by averaging over all the nonequilibrium trajectories.

In these figures, the circle symbol denotes data from direct NEMD, and the triangle symbol denotes data from TTCF. We also plot the statistical error bars, taken as the standard error.

From Figure 8.1, we can see that the results from direct NEMD and TTCF are consistent. The results from direct NEMD are more accurate than that from TTCF at this shear rate. The TTCF results have larger error bars and fluctuate more rapidly.

We can also see that the normal elements of the pressure tensor P_{xx} , P_{yy} and P_{zz} are not all equal. By averaging over the steady-state regions, we can obtain these values and hence the first normal stress difference N_1 and the second normal stress difference N_2 .

$$P_{xx} = 7.2359 \pm 0.0002$$

$$P_{yy} = 7.2745 \pm 0.0005$$

$$P_{zz} = 6.9183 \pm 0.0002$$

$$N_1 \equiv P_{xx} - P_{yy} = -0.0386 \pm 0.0007$$

$$N_2 \equiv P_{yy} - P_{zz} = 0.3562 \pm 0.0007$$

We can define the relaxation time as the time needed for the system to evolve from the instant we apply a shear force to the moment the system reaches a nonequilibrium steady

state. We can regard the last 500 time steps as a steady state. We can estimate the relaxation time by fitting a line $B(t) = C$, where C is a constant and $B(t)$ is the phase variable, within this steady state region and finding its intercept with the decaying function $B(t)$ at earlier times. We estimate the relaxation time to be approximately 0.67. We also observe normal stress overshoots as we would expect for such a relatively large strain rate.

In Figure 8.2 we plot analogous results at a small shear rate of 0.002. In order to get more accurate results in this weak field, we simulated for very long times. We ran four equilibrium trajectories, where each trajectory has 2500×100000 time steps. From each equilibrium trajectory, 200000 nonequilibrium trajectories are initiated. Because of the weaker field we increase the integration time step to 0.002. The system is composed of 500 particles.

At this smaller shear rate, we estimate the relaxation time to be 1.25, but we cannot observe any normal stress overshoot. We also calculate the first and second normal stresses:

$$P_{xx} = 6.4001 \pm 0.0001$$

$$P_{yy} = 6.40008 \pm 0.00004$$

$$P_{zz} = 6.39966 \pm 0.00005$$

$$N_1 \equiv P_{xx} - P_{yy} = 0.0000 \pm 0.0001$$

$$N_2 \equiv P_{yy} - P_{zz} = 0.0004 \pm 0.0001$$

By comparing to the $\dot{\gamma} = 1$ case, we note some standard conclusions. The larger the strain rate, the larger the normal stress differences. This is to be expected because the normal stress differences reflect nonlinear phenomena. The larger the strain rate, the more apparent the dilatancy (the shear-induced increase of normal stresses). The larger the strain rate, the larger magnitude of overshoot. But the larger the strain rate, the shorter the relaxation time.

Using these results, we can compare direct NEMD and our TTCF calculations for $\dot{\gamma} = 0.002$ by comparing their error bars. In contrast to the $\dot{\gamma} = 1$ case, the results of our

TTCF calculations are more accurate than those of direct time-averaging NEMD. The TTCF results have small error bars and vary smoothly with time. The direct NEMD results have large error bars and fluctuate more rapidly.

From our simulations it is clear that there exists a critical shear rate, above which direct time-averaging is more accurate than TTCF, and below which TTCF is the statistically superior methodology. From our WCA simulations we estimate this value at $\dot{\gamma} \approx 0.05$, though we do not present all the data here, as it is too much to display.

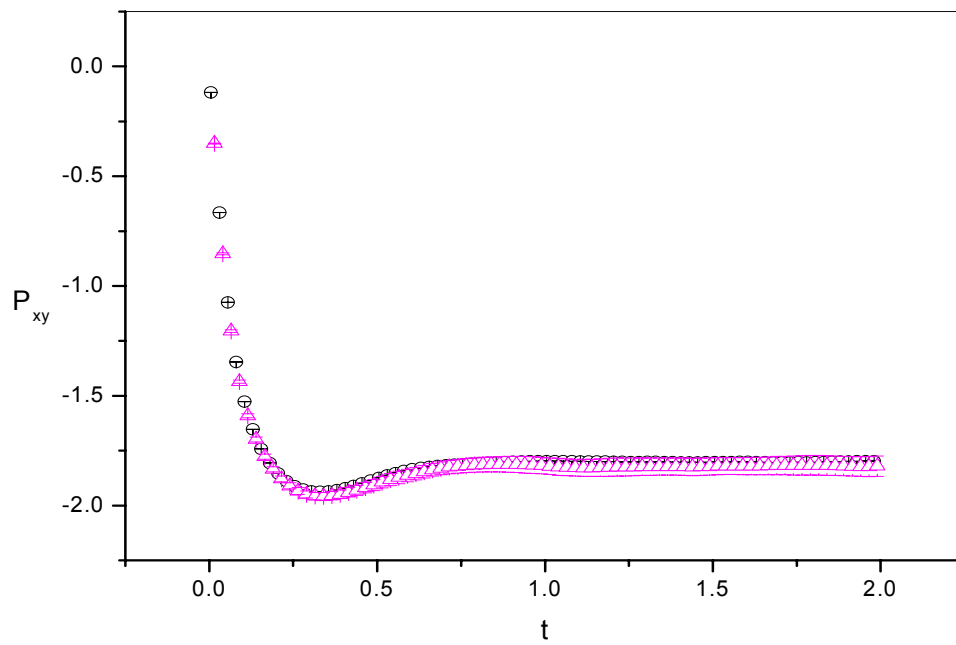


Figure 8.1 (a) P_{xy} as a function of time at shear rate $\dot{\gamma}=1$. Circle symbols are direct NEMD data, while triangle symbols are TTCF data.

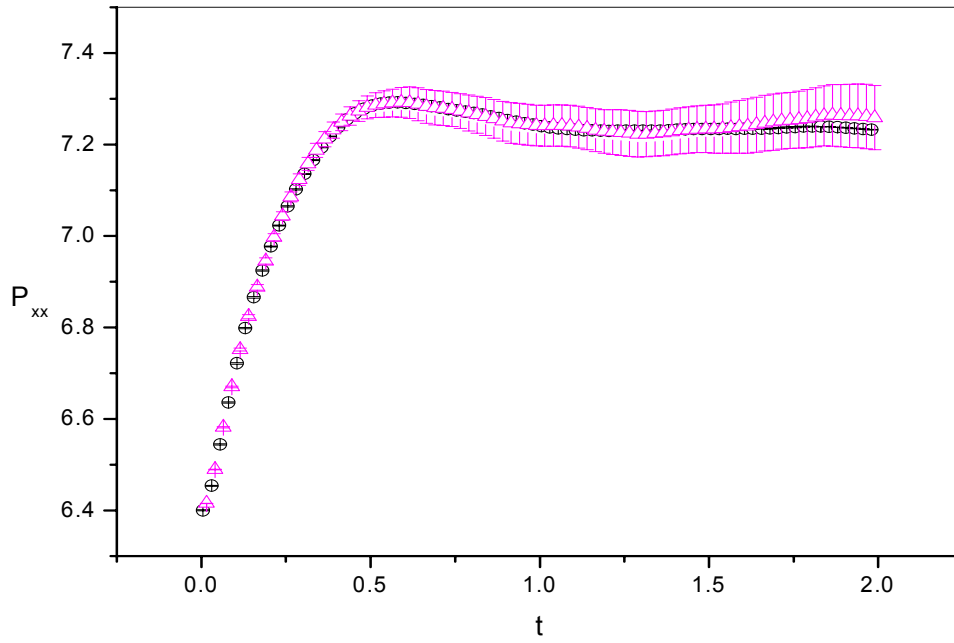


Figure 8.1 (b) P_{xx} as a function of time at shear rate $\dot{\gamma} = 1$.

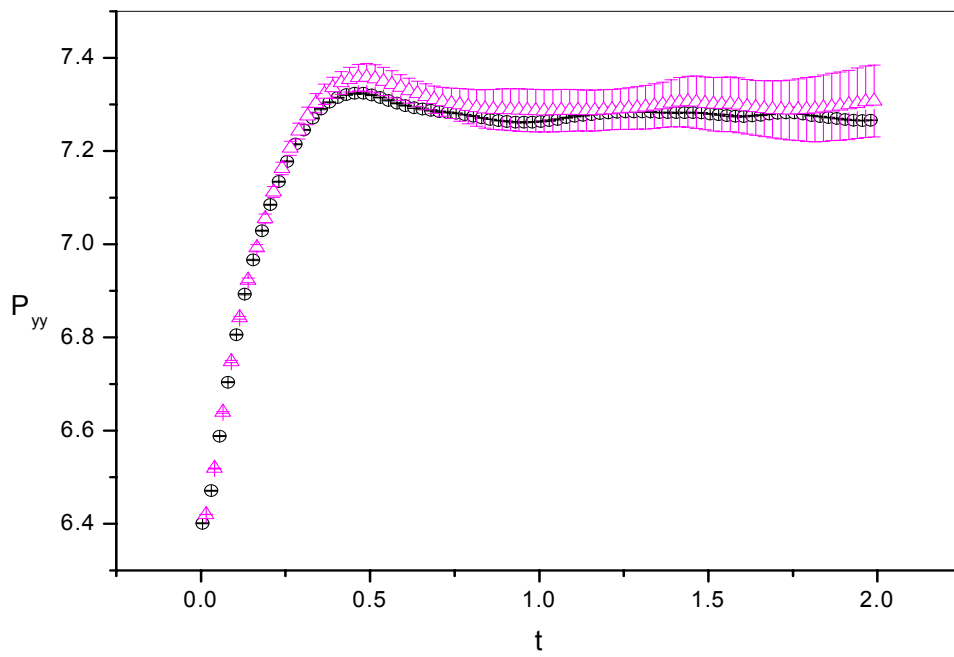


Figure 8.1 (c) P_{yy} as a function of time at shear rate $\dot{\gamma} = 1$.

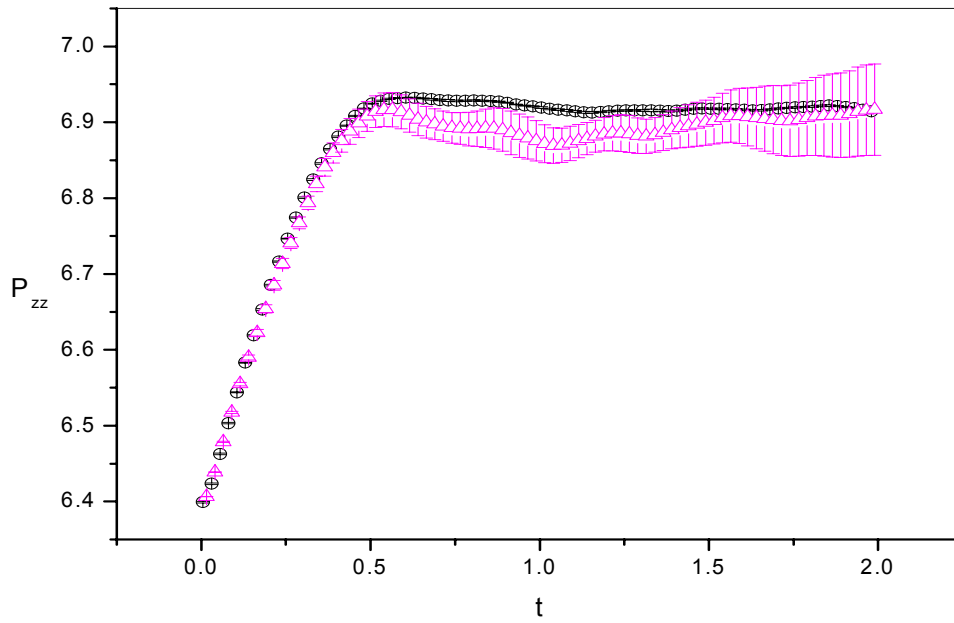


Figure 8.1 (d) P_{zz} as a function of time at shear rate $\dot{\gamma} = 1$.

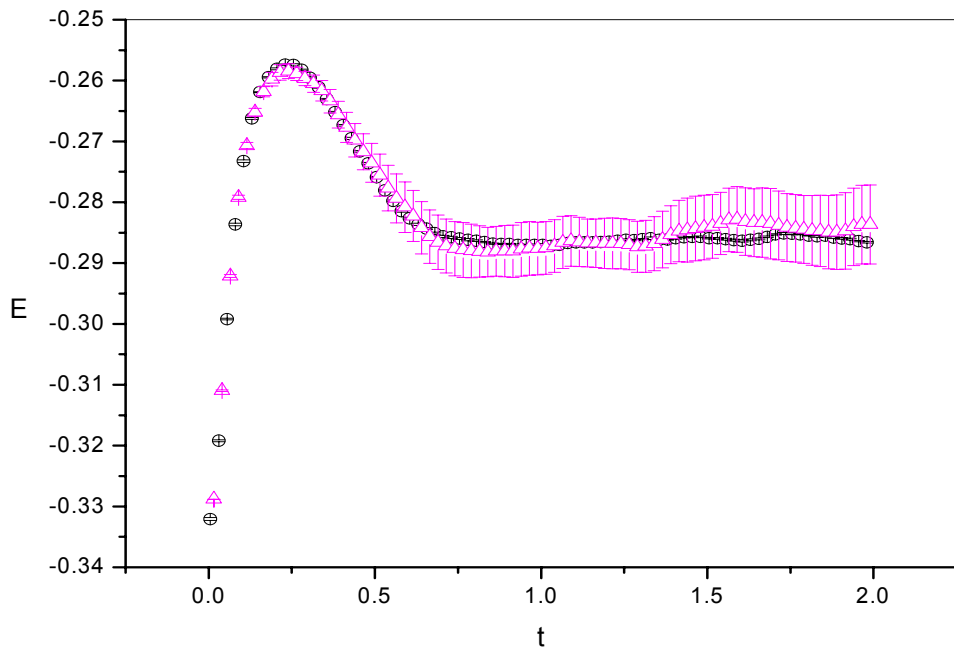


Figure 8.1 (e) E as a function of time at shear rate $\dot{\gamma} = 1$.

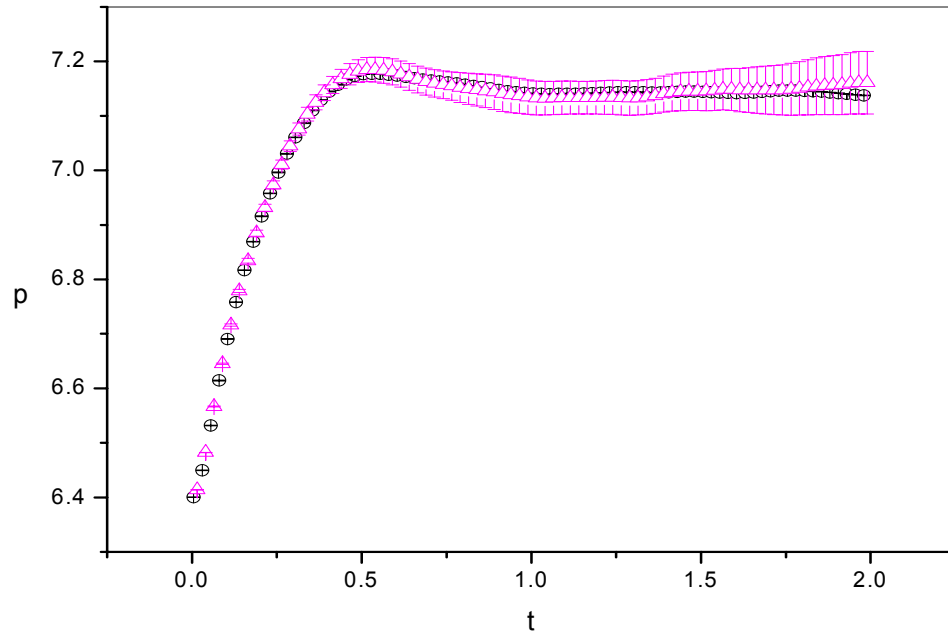


Figure 8.1 (f) p as a function of time at shear rate $\dot{\gamma} = 1$.

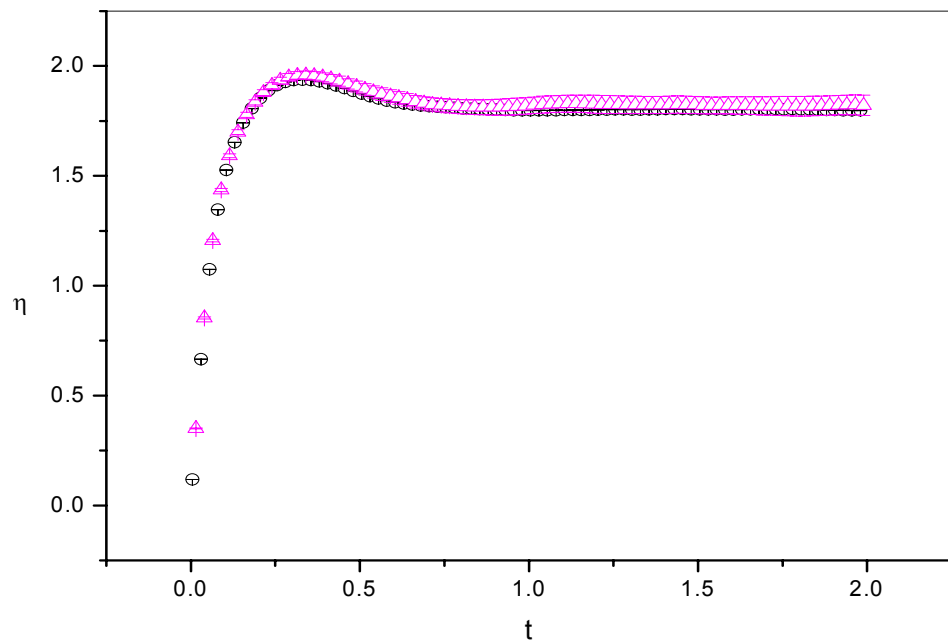


Figure 8.1 (g) η as a function of time at shear rate $\dot{\gamma} = 1$.

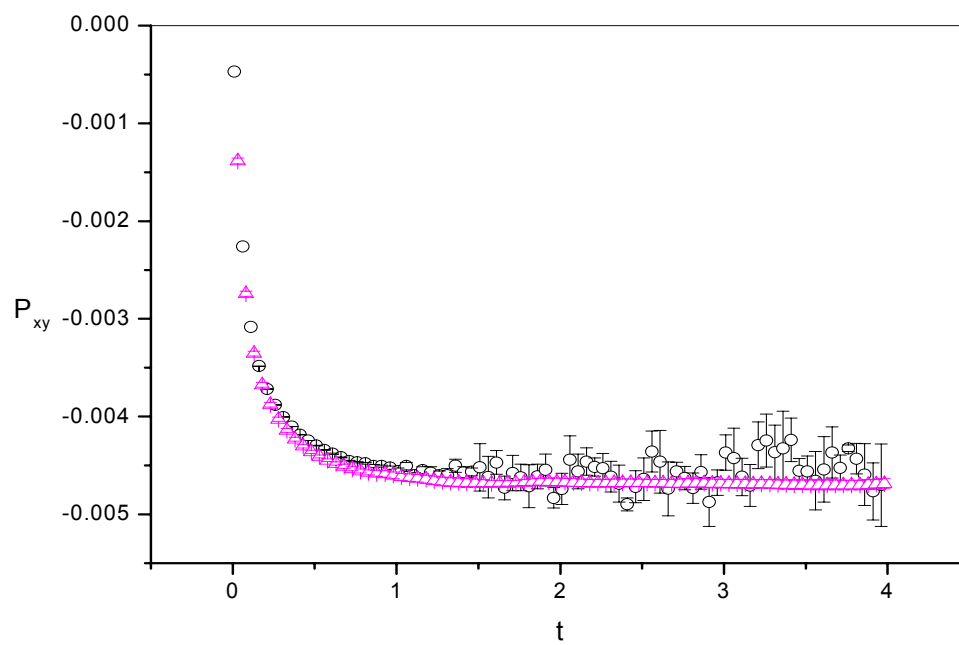


Figure 8.2 (a) P_{xy} as a function of time at shear rate $\dot{\gamma} = 0.002$. Circle symbols are direct NEMD data, while triangle symbols are TTCF data.

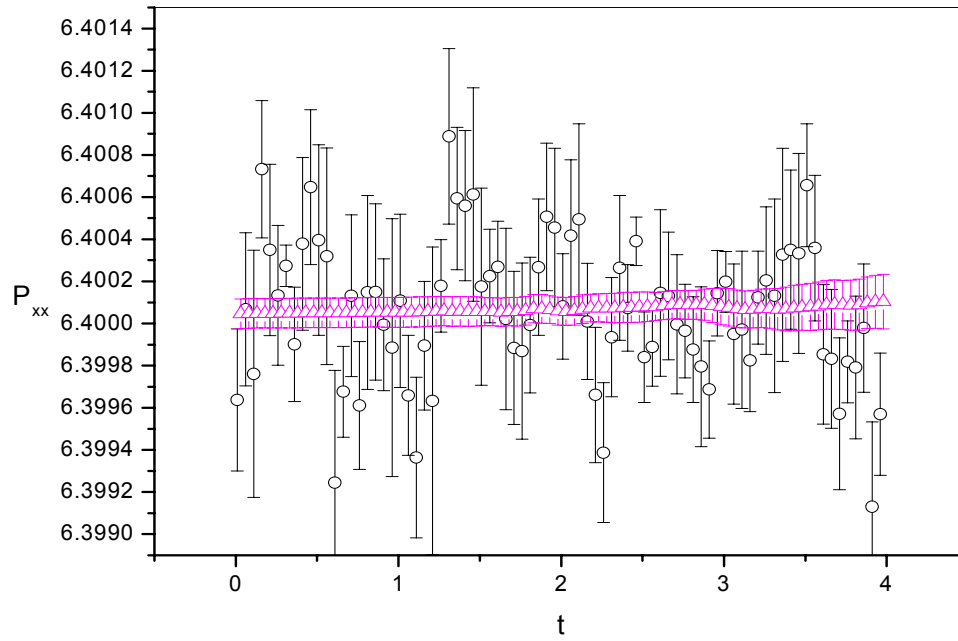


Figure 8.2 (b) P_{xx} as a function of time at shear rate $\dot{\gamma}=0.002$.

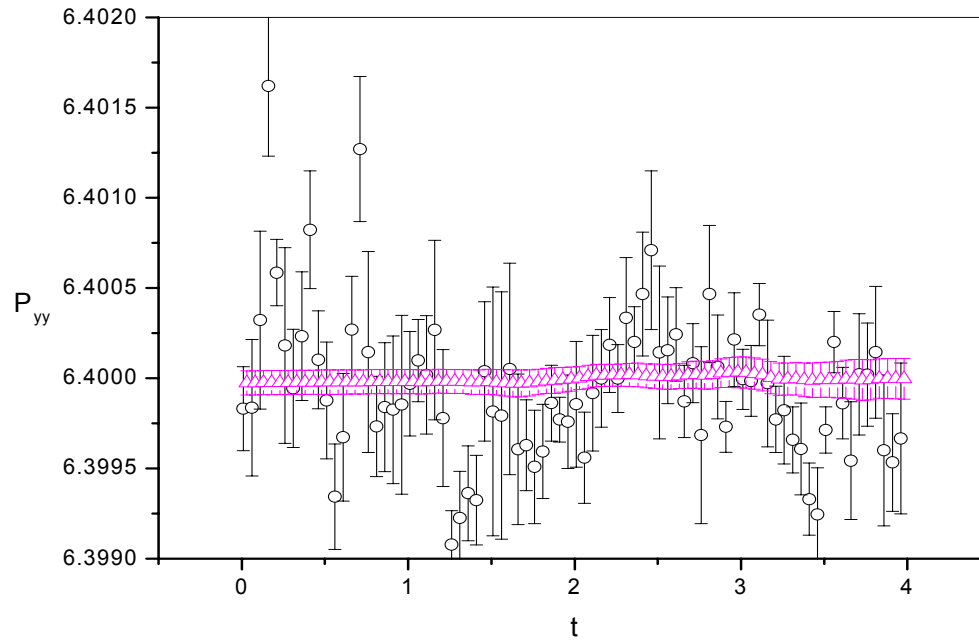


Figure 8.2 (c) P_{yy} as a function of time at shear rate $\dot{\gamma}=0.002$.

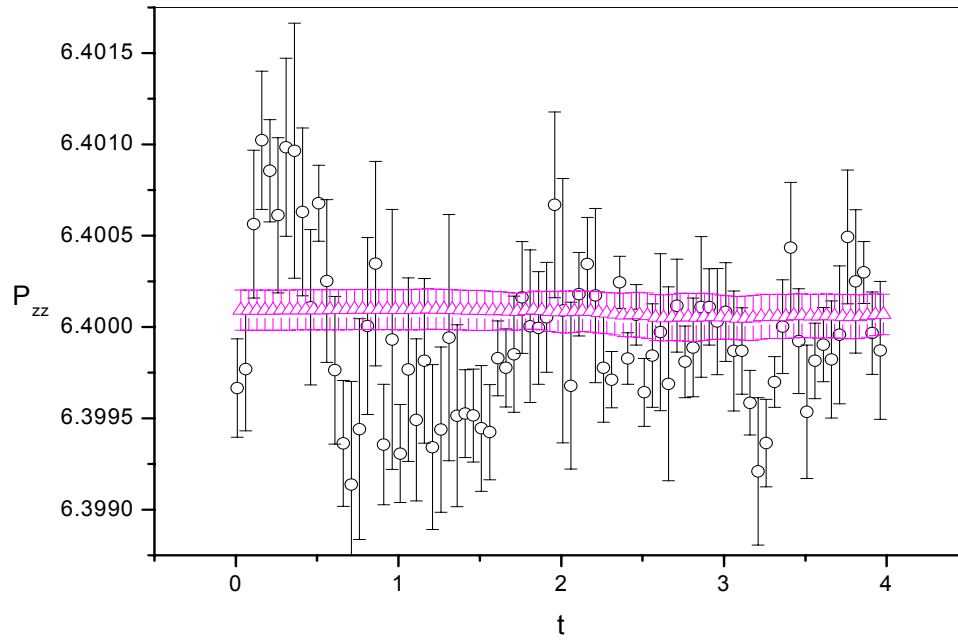


Figure 8.2 (d) P_{zz} as a function of time at shear rate $\dot{\gamma}=0.002$.

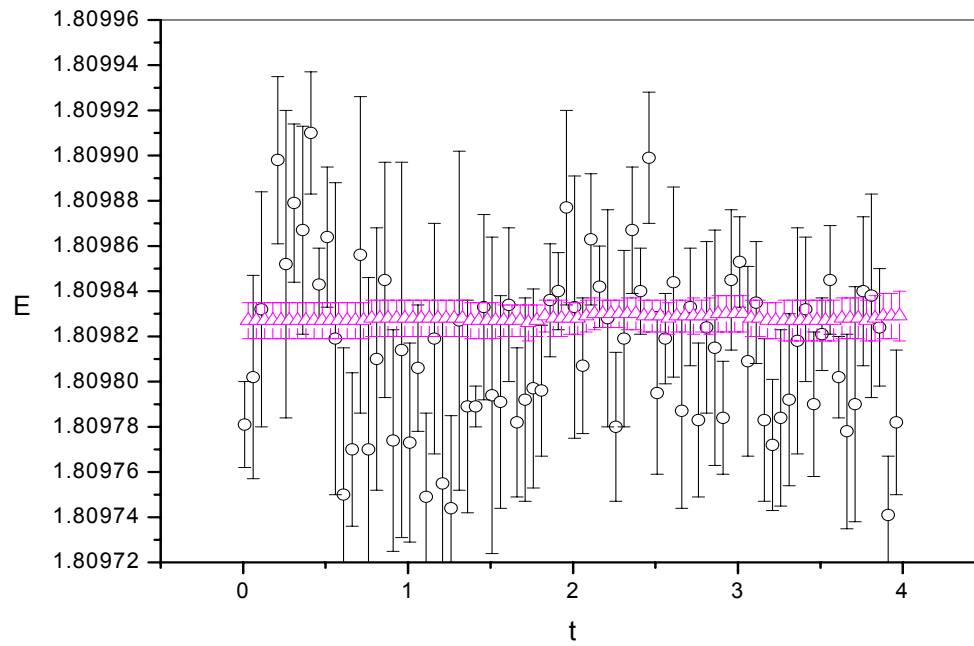


Figure 8.2 (e) E as a function of time at shear rate $\dot{\gamma}=0.002$.

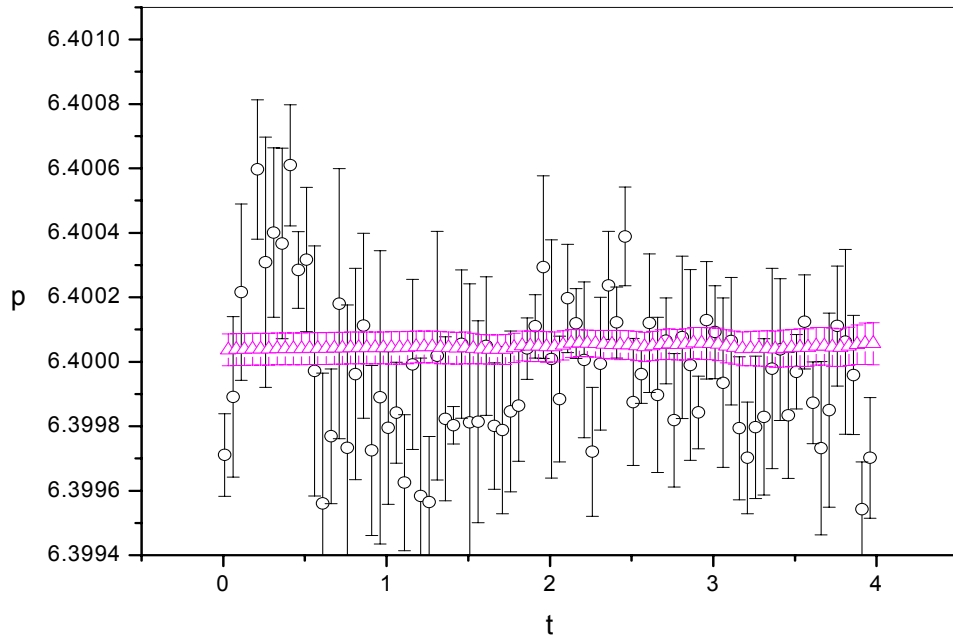


Figure 8.2 (f) p as a function of time at shear rate $\dot{\gamma}=0.002$.

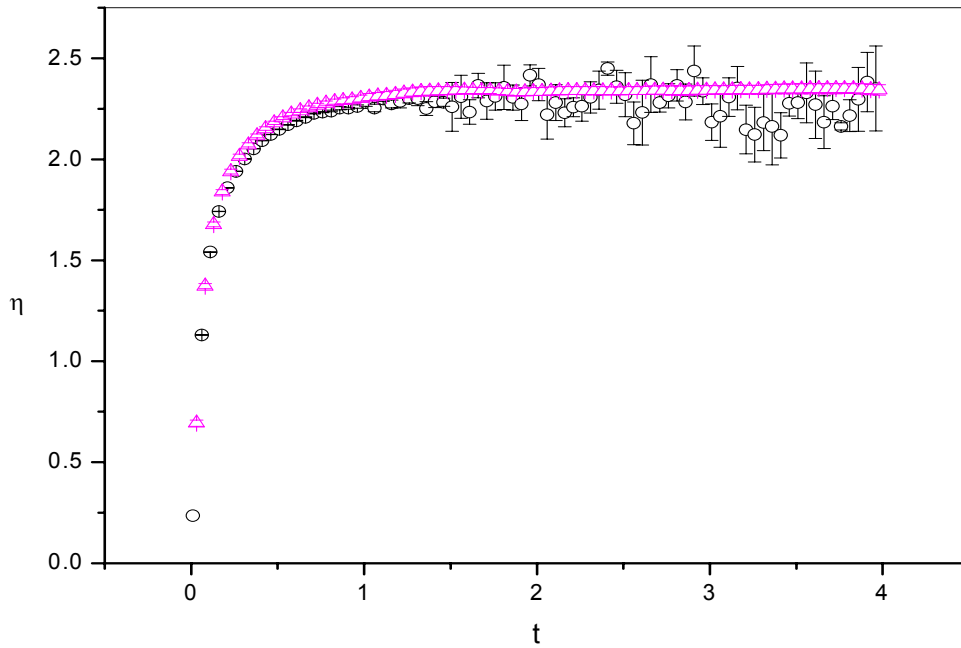


Figure 8.2 (g) η as a function of time at shear rate $\dot{\gamma}=0.002$.

8.4. Viscosity at small shear rate

Most calculations of the viscosity of fluids obtained by NEMD simulation involve direct time-averaging, which is limited to the high field region. For simple atomic fluids this is limited to $\sim \dot{\gamma} > 10^{-2}$. By using the TTCF method, we focus on the shear rate range of order 10^{-3} . We calculated the viscosity at $\dot{\gamma} = 0.002, 0.004, 0.006, 0.008, \text{ and } 0.01$. Motivated by our mode coupling theory investigations we are interested to investigate if the viscosity has any measurable trends in this weak field regime.

Our simulation details are the same as those in Figure 8.2. For every shear rate, we run equilibrium simulations of $4 \times 2500 \times 100000$ time steps, plus additional nonequilibrium simulations for $4 \times 2000 \times 200000$ time steps.

Figures 8.3 and 8.4 show the shear stress vs. time and shear stress vs. shear rate respectively. Because the error bars are the size of the symbols, we do not plot them. From these figures, we can see that the relation between shear stress and shear rate is linear. The value of the correlation coefficient is: $R = 0.99976$. This implies that the shear stress is proportional to shear rate, which is just the definition of a Newtonian fluid. From the linear fit we obtain a slope, and hence the viscosity, $\eta = 2.30 \pm 0.03$.

Using the TTCF method, we have demonstrated that in the $\dot{\gamma} \leq 0.01$ region, viscosity does not change with shear rate, and the WCA fluid is Newtonian. Our results agree with those of Borzsak, *et al.* [Bor02] and Bhupathiraju *et al.* [Bhu96] within error bars. We note here that our simulations were performed simultaneously and independently of Borzsak *et al.* As many of our results are identical to theirs we do not devote much detail to their discussion. We also point out that due to lack of time we were unable to probe the weak field non-Newtonian regime $0.01 \leq \dot{\gamma} \leq 0.1$, which is where comparisons to mode coupling theory may be most meaningful.

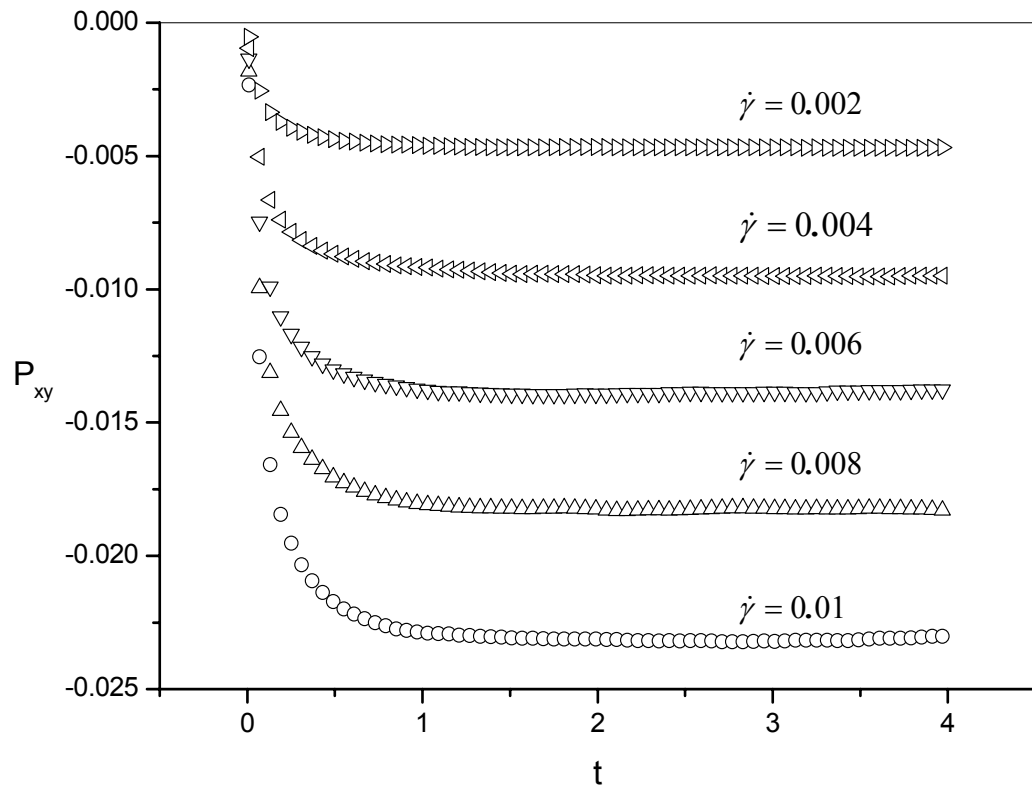


Figure 8.3 Shear stress vs. time.

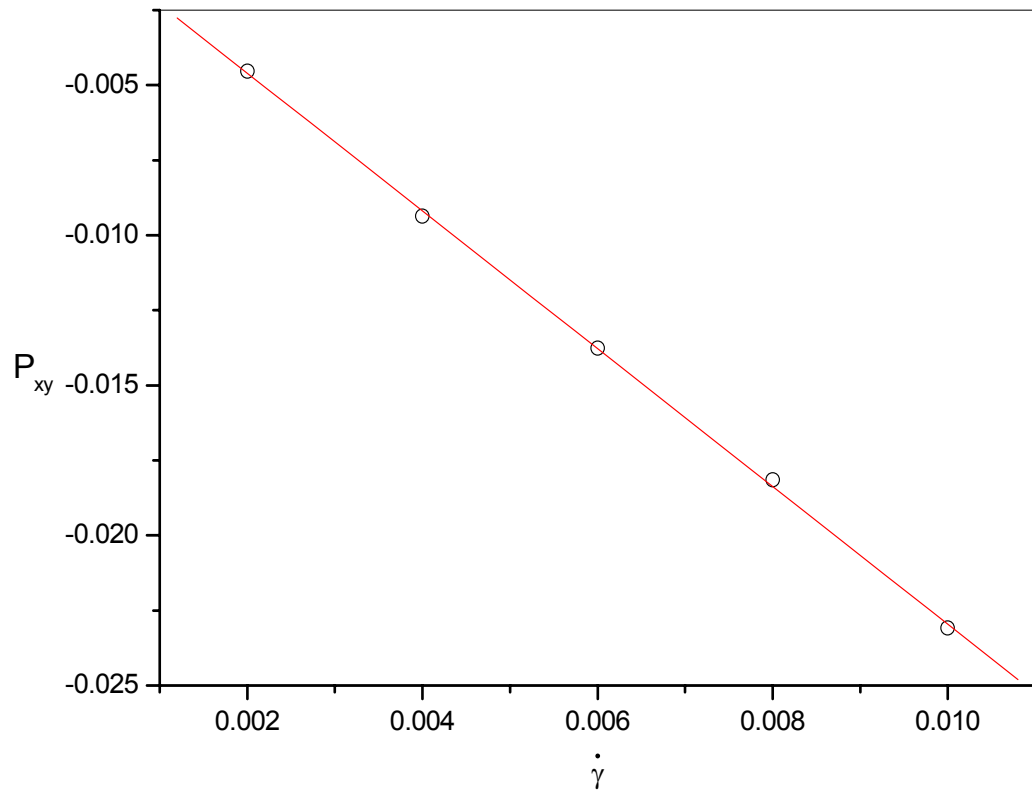


Figure 8.4 Shear stress vs. shear rate.

8.5. The long-time tail

The long-time tail problem is of considerable significance [Eva80b, Fox83]. From the point of view of computer simulations, the long-time tail affects the accuracy of simulation results in the long time limit. As we know, when one uses the Green-Kubo relations to calculate the transport coefficients, the problem becomes an evaluation of a time autocorrelation function. For example, to calculate the diffusion coefficient, one needs to calculate the velocity autocorrelation function. If the integrand decays with time quickly, then one can truncate the time integration earlier to get an enough accurate result.

Now we consider the decay with time of the time autocorrelation functions for the shear stress. This correlation function is related to the computation of the viscosity. Very often, when one speaks of a long-time tail, one implies using the Green-Kubo relations, where the system is in equilibrium. In the case of shear flow, the system is in a nonequilibrium state, and one can use the TTCF algorithm to calculate the viscosity. From the TTCF Eqn. (8.2) we can see that any phase variable B can be expressed by a time correlation function $\langle B(t)P_{xy}(0) \rangle$. Here, $P_{xy}(0)$ is a value of the shear stress at $t = 0$ at equilibrium. $B(t)$ is any nonequilibrium phase variable. We carried out nonequilibrium molecular dynamics simulations at two different state points with the same shear rate, $\dot{\gamma} = 0.01$. The two state points are: $(T, \rho) = (0.722, 0.8442)$, and $(0.722, 0.72)$ respectively. The simulation details are same as in Section 8.4.

Our results are shown in Figures 8.5 and 8.6. Because the error bars are the size of symbols, as before, we do not plot them. In these Figures, we also fit the time correlation functions with three different functions. These are: a power law with the exponent a fixed value $-3/2$, a variable power exponent α , and an exponential function.

From these functional fits we can see that the well known long-time tail decaying function $t^{-3/2}$ does not fit the data best. Instead, a exponential function seems to fit the data best. However, when we use a power law with an exponent larger than $3/2$ (for example, at state points $(T, \rho) = (0.722, 0.8442)$ and $(0.722, 0.72)$, we use 1.60 and 2.88 respectively), the goodness of the fits are very close to that of the exponential function. We found that this conclusion will not be affected by changing the state point.

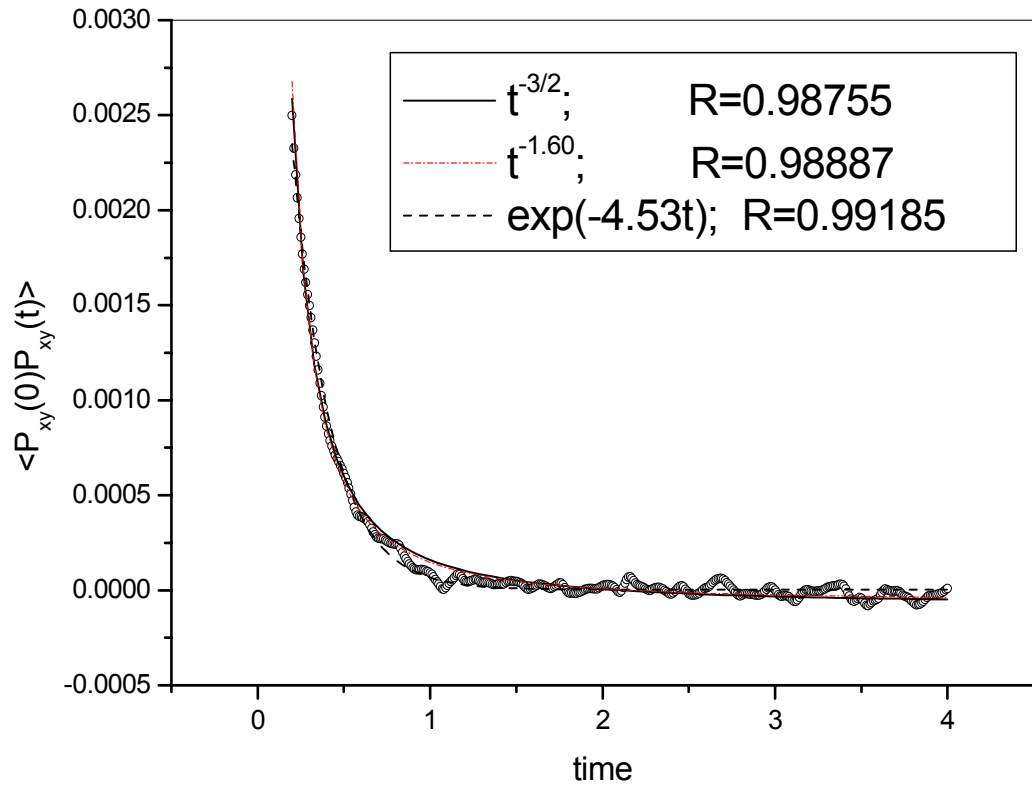


Figure 8.5 Time correlation function $\langle P_{xy}(0)P(t) \rangle$ at the Lennard-Jones triple point with a shear rate of $\dot{\gamma} = 0.01$.

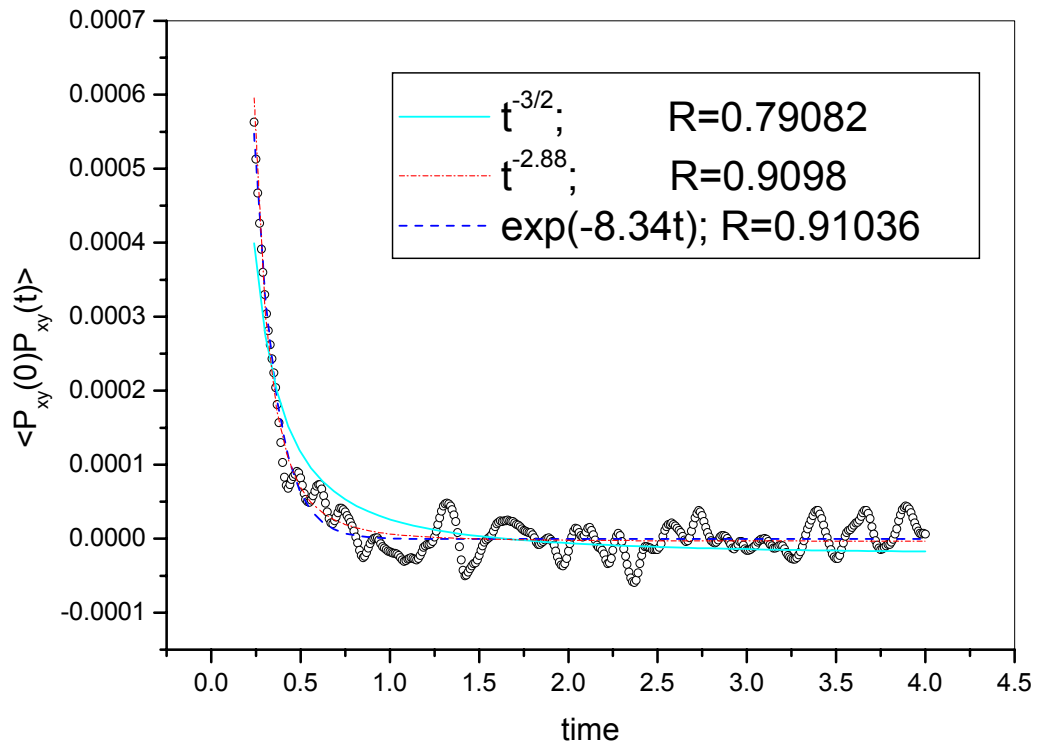


Figure 8.6 Time correlation function $\langle P_{xy}(0)P(t) \rangle$ at the state point $(T, \rho) = (0.722, 0.72)$ with a shear rate of $\dot{\gamma} = 0.01$.

8.6. Conclusions

Our simulation results confirm that in the strong field case direct time-averaging NEMD is more effective than the TTCF method, though their results are consistent within errors. In the weak field limit, TTCF is superior. There exists a critical shear rate where if the field is stronger than this value, direct NEMD is most efficient. If the field is weaker than this value, one should use TTCF. For the WCA system, this value is about $\dot{\gamma} = 0.05$. We also demonstrated that in the region of shear rate smaller than 0.01, the WCA fluid is Newtonian.

For the nonequilibrium stress-stress time correlation functions, the long-time tail $t^{-3/2}$ is not conclusively observed. A decaying exponential fits the data better. But with an exponent larger than $3/2$, a power law function can get a goodness of fit very close to that of the exponential function. More work is required to more confidently resolve this issue.